



## Modeling of the heat transfer performance of plate-type dispersion nuclear fuel elements

Shurong Ding\*, Yongzhong Huo\*, XiaoQing Yan

Department of Mechanics and Engineering Science, Fudan University, Shanghai 200433, PR China

### ARTICLE INFO

#### Article history:

Received 18 July 2008

Accepted 21 April 2009

### ABSTRACT

Considering the mutual actions between fuel particles and the metal matrix, the three-dimensional finite element models are developed to simulate the heat transfer behaviors of dispersion nuclear fuel plates. The research results indicate that the temperatures of the fuel plate might rise more distinctly with considering the particle swelling and the degraded surface heat transfer coefficients with increasing burnup; the local heating phenomenon within the particles appears when their thermal conductivities are too low. With rise of the surface heat transfer coefficients, the temperatures within the fuel plate decrease; the temperatures of the fuel plate are sensitive to the variations of the heat transfer coefficients whose values are lower, but their effects are weakened and slight when the heat transfer coefficients increase and reach a certain extent. Increasing the heat generation rate leads to elevating the internal temperatures. The temperatures and the maximum temperature differences within the plate increase along with the particle volume fractions. The surface thermal flux goes up along with particle volume fractions and heat generation rates, but the effects of surface heat transfer coefficients are not evident.

© 2009 Elsevier B.V. All rights reserved.

### 1. Introduction

The Reduced Enrichment for Research and Test Reactors (RERTR) program started in 1978. This program has been tasked with the conversion of research reactors from highly enriched to low-enriched uranium (LEU) with a  $^{235}\text{U}$  content of less than 20%. Many countries have been seeking for technical means to achieve this goal [1]. In order to reach the requisite power density, the needs to raise the density of the exiting fuels must be met. Due to the high uranium density of dispersion nuclear elements [2], several kinds of dispersion fuels such as  $\text{U}_3\text{Si}_2$  dispersion fuel are formally qualified for reactor use and a good many research and test reactors have been converted to LEU fuels. However, there remain some reactors that have not been converted to LEU fuels because the initial developed dispersion fuels might not meet the needs of the required high power density. A range of high-density advanced dispersion fuels such as the U–Mo dispersion fuel plates are being developed and a series of irradiation tests [3–6] are being implemented.

Dispersion fuels are composed of fissile particles and metal matrix with fissile particles dispersed in the non-fissile metal matrix. They are similar to particle composites in the configurations and they are designable. The performances of the dispersion fuels are affected by several factors, for example, the geometries, the sizes,

the volume fractions and the distribution forms of the fissile particles, and the material properties of the particles and the metals, etc. The thermal and mechanical behaviors of the dispersion fuel elements during their lifetime under different operating conditions need to be evaluated.

In order to design high performance dispersion fuel elements, irradiation tests are necessary. However, such tests are very time-consuming and it is impossible to carry out tests for all the circumstances. Thus, numerical modeling is becoming a measure of importance, which might help to understand better the irradiation experiments of dispersion fuel elements and explain the damage mechanism. Other purposes are to perform parametric studies to identify the more sensible parameters on the performances of fuel elements. Thus, numerical simulation might be a support to the fuel design.

Rest and Hofman [7] developed some modeling researches on fuel swelling: they adopted the spherical symmetry model without considering the mutual actions among fuel particles. Lately, in order to analyze the mutual action among the fuel particles more precisely, the numerical modeling for the rod-type dispersion fuel elements using fem considering more actual particle distribution was presented [2]. The relative researches on dispersion fuel plate also came forth and some specific codes for the thermal and thermal–mechanical analysis were developed and were being upgraded, including FASTDART [8,9], PLATE [10,11], MAIA [12,13] and DART-TM [14] and so on. In these studies, the dispersion fuel meat was generally treated as homogeneous and the modeling

\* Corresponding authors.

E-mail addresses: [dsr1971@163.com](mailto:dsr1971@163.com) (S. Ding), [yzhuo@fudan.edu.cn](mailto:yzhuo@fudan.edu.cn) (Y. Huo).

was one-dimensional or two-dimensional, that is, the mutual actions between fuel particles and the matrix and the mutual actions among fuel particles are not taken into account.

In this study, allowing for the mutual actions between fuel particles and the metal matrix and the ones among the fuel particles, the three-dimensional finite element models suitable for the plate-type dispersion fuel elements are developed, with which the effects of the in-pile conditions on the behaviors of fuel plates might also be investigated. And the heat transfer behaviors of dispersion fuel plates are mainly modeled in this study.

## 2. Basic formulas

The heat generated by nuclear fissions of the fuel particles might lead to the temperature variations of the dispersion fuel elements. It is of importance to determine the temperature field because it affects the thermal–mechanical behaviors of the dispersion fuel elements owing to the temperature-dependence of the mechanical parameters of the fuel particles and the matrix material.

The thermal conductivity of the fuel particle might degrade with increasing burnup on account of the generated solid and gaseous fission products [2], so the whole lifetime should be divided into many time steps and thus it might be treated as a steady-state thermal exchange problem at every time step.

### 2.1. The steady-state heat exchange equation and the boundary conditions

The steady-state heat exchange equation is given as

$$\nabla \cdot (k(T)\nabla T) + \dot{q} = 0, \quad (1)$$

where  $k$  is the thermal conductivity, whose unit is W/m K;  $T$  is the temperature, whose unit is K and  $\dot{q}$  is the heat generation rate, whose unit is W/m<sup>3</sup>.

In order to determine the temperature field of the dispersion nuclear fuel element, the boundary condition, the thermal conductivities of the fuel particles and the matrix material, the irradiation swelling of the fuel particles and the heat generation rate of the nuclear fuel particles should be defined.

The three kinds of boundary conditions are as follows

$$T = g(x, y, z), \quad (2)$$

$$-k \frac{\partial T}{\partial n} = f(x, y, z), \quad (3)$$

$$-k \frac{\partial T}{\partial n} = h(T - T_f), \quad (4)$$

where Eq. (2) denotes that the boundary temperature is known; Eq. (3) describes that the thermal flux along the external normal direction is known and  $n$  expresses the external normal direction; Eq. (4) shows the convection boundary condition, in which  $h$  is the heat transfer coefficient and  $T_f$  is the temperature of the periphery liquid.

### 2.2. Thermal conductivities of fuel particles and matrix

The model of thermal conductivities of fuel particles improved by Lucuta et al. [15] consists of five contributions and can be expressed as

$$k = k_0 \cdot \text{FD} \cdot \text{FP} \cdot \text{FM} \cdot \text{FR}, \quad (5)$$

where:

$$k_0 = \frac{1}{0.0375 + 2.165 \times 10^{-4}T + \left[ \frac{4.715 \times 10^9}{T^2} \right] \exp\left(-\frac{16361}{T}\right)}. \quad (6)$$

And it is Harding's expression for the thermal conductivity of unirradiated UO<sub>2</sub>; FD quantifies the effect of dissolved fission products; FP describes the effect of precipitated solid fission products; FM is the modified Maxwell factor for the effect of the pore and fission-gas bubbles; FR characterizes the effect of radiation damage.

$$\text{FD} = \left[ \frac{1.09}{B^{3.265}} + \frac{0.0643}{\sqrt{B}} \sqrt{T} \right] \arctan \left[ \frac{1}{\frac{1.09}{B^{3.265}} + \frac{0.0643}{\sqrt{B}} \sqrt{T}} \right],$$

$$\text{FP} = 1 + \left( \frac{0.019B}{3 - 0.019B} \right) \left[ \frac{1}{1 + \exp\left(-\frac{T-1200}{100}\right)} \right]$$

$$\text{FM} = \frac{1 - P}{1 + (s - 1)P}, \quad \text{FR} = 1 - \frac{0.2}{1 + \exp\left(\frac{T-900}{80}\right)}$$

In the above expressions:  $T$  represents the temperature in Kelvin.  $B$  is the burnup in at.%.  $P$  is the volume fraction of the pores and bubbles.  $s$  is the pore shape factor (with a value of 1.5 for spherical bubbles in the absence of other data).

For the Zircaloy matrix, its thermal conductivity from the room temperature to the melting point can be expressed by [16]:

$$k = 7.51 + 2.09 \times 10^{-2}T - 1.45 \times 10^{-5}T^2 + 7.67 \times 10^{-9}T^3. \quad (7)$$

### 2.3. The heat generation rates of the fuel particles

The heat generation rate of the fuel particles corresponds to their fission rate. For a certain fission rate, considering that one time nuclear fission emits 200 MeV heat energy and  $1 \text{ eV} = 1.602 \times 10^{-19} \text{ J}$ , the corresponding heat generation rate might be calculated. The computation equation is obtained as Eq. (8)

$$\dot{q} = c \cdot \dot{f}, \quad (8)$$

where  $c = 3.204 \times 10^{-11} \text{ J/fission}$  is the generated heat energy every fissioning event and  $\dot{f}$  is the fission rate of the fuel particles, which depicts the fission numbers per time per volume of the fuel particles.

### 2.4. Fuel particle swelling

The fuel particle swelling is usually characterized by the relative volume variations. A kind of swelling coefficient  $\beta_V$  can be introduced as the volume swelling rate by

$$\text{SW}(\text{BU}) = \frac{\Delta V}{V_0} = \int_0^{\text{BU}} \beta_V d(\text{BU}), \quad (9)$$

where  $V_0$  is the reference volume,  $\Delta V$  is the volume variation measured after a period of fission reactions. BU is called the burnup with the unit %FIMA, which is defined as the ratio of the number of the fissioned U atoms to the original number of U atoms and is widely used to characterize the extent of the fission reactions in the nuclear fuel.

The swelling rate  $\beta_V$  (swelling per %FIMA) has three contributions from the fission-gas bubbles  $\beta_V^{\text{gs}}$ , the solid fission product  $\beta_V^{\text{ss}}$  and the fission densification  $\beta_V^{\text{ds}}$ . Namely

$$\beta_V = \beta_V^{\text{gs}} + \beta_V^{\text{ss}} + \beta_V^{\text{ds}}. \quad (10)$$

All the swelling rates have been studied extensively in the literatures and are generally rather complicated. For our FEM calculations, the following simplified relations [17–19] for UO<sub>2</sub> in PWRs will be used

$$\beta_V^{\text{gs}} = 1.122 \times 10^3 \exp(-1.645 \times 10^4 / (T - 100)), \quad (11)$$

$$\beta_V^{\text{ss}} = 6.4 \times 10^{-3}, \quad (12)$$

$$\beta_V^{\text{ds}} = -[0.51 \exp(-59.9 \times \text{BU}) + 4.76 \times 10^{-2} \exp(-10.07 \times \text{BU})], \quad (13)$$

where  $T$  is the temperature, whose unit is K. Note that  $\beta_V^{gs}$  is temperature-dependent and  $\beta_V^{ds}$  is burnup-dependent.

### 3. The finite element model

In this paper, the plate-type dispersion nuclear fuel element is considered. As shown in Fig. 1, the thickness of the fuel plate (1.24 mm) is far smaller than its length and width. Thus the generated heat energy is mainly transferred out by the coolant water through the upside and downside surfaces. So, the upside and downside surfaces are the main boundaries of the dispersion fuel plate. The relative boundary conditions might play an important role in the temperature field of the fuel plate. Thus the selected finite element model should include the main boundary and the relative boundary conditions should be reflected. And the internal micro-structure of the dispersion nuclear fuel should also be considered because the effects of the fuel particles and the matrix on the thermal performance are to be evaluated. It is a crucial problem how to develop the three-dimensional finite element model for the concerned study.

Since the dispersion nuclear fuel is similar to the particle composite in the framework, the meso-mechanics research thought [20,21] of the particle reinforced composites might be used for reference. In the particle composite, the method of Representative Volume Element (RVE) [20,21] is usually adopted. But the RVE method assumes that the size of the particle is much smaller than the studied object scale to solve the equivalent material moduli of the macroscopic homogeneous material corresponding to the meso-structures, so the particles are supposed to be periodically distributed and only the periodic RVE might be selected as the finite element model. This method might not be directly applied to the dispersion nuclear fuel plate for the following two reasons: firstly, the thickness of the fuel plate is very thin and is only several millimeters, which is not much larger than the average diameter (several hundred microns) of the fuel particles; secondly, the surface boundary conditions might have remarkable effects on the temperature distributions of the fuel plate so that the actual boundary conditions at the upside and downside surfaces should be considered.

A specific RVE is proposed, as illustrated in Fig. 1. This method of choosing the finite element model assumes that the fuel particles are periodically distributed along the length and width directions, thus the selected finite element model adopts periodical sizes (meso-scale) at the length and width direction and makes use of the actual size (macro-scale) along the thickness direction. So, this kind of RVE model might be called two-scale model. The fuel particles might have different distribution fashions along the length or width direction and might be random distribution, so one can investigate the effects of different distributions on the thermal-mechanical behaviors. The distribution of the fuel particles along the thickness might be arbitrary. In the actual modeling, the idiographic finite element model should be developed according to the volume fraction  $V_f$ , the diameter  $d$  and the distribution characters of the fuel particles.

First of all, a simple case is considered. Supposing that the spherical fuel particles ( $d = 100 \mu\text{m}$ ) are cubically arranged in the matrix, the developed RVE is shown as Fig. 2(a) and the chosen fi-

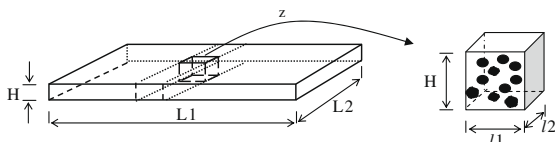


Fig. 1. Dispersion fuel plate and the representative plate element.

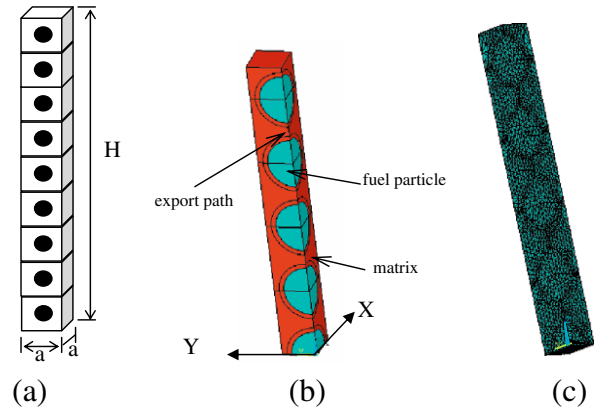


Fig. 2. The RVE (a), finite element model (b) and the mesh figure (c) of the dispersion fuel plate for the cubic distribution case.

nite element model is constructed in accordance with symmetries, as displayed in Fig. 2(b). The plane with  $Z = 0$  expresses the mid-plane of the fuel plate and the plane with  $Z = H/2$  denotes the upside surface which is the contact surface with the coolant water.

The boundary conditions are as the following:

- (1) At the planes  $X = 0$ ,  $X = a/2$ ,  $Y = 0$ ,  $Y = a/2$  and  $Z = 0$ , the adiabatic boundary condition should be applied because they are the symmetrical planes. Eq. (3) is suitable:  $-k \frac{\partial T}{\partial n} = 0$ .
- (2)  $Z = H/2$  plane is the convection boundary, the relative boundary condition is expressed as Eq. (4).
- (3) At the interfaces between the fuel particles and the matrix:  $T_p = T_m$ ,  $-k_p \frac{\partial T_p}{\partial n} = -k_m \frac{\partial T_m}{\partial n}$ , where  $T_p$ ,  $T_m$  are the temperatures and  $\kappa_p$ ,  $\kappa_m$  are the thermal conductivities of the particle and the matrix, respectively. That is, the temperatures and the thermal fluxes along the normal directions of the interfaces are continuous.

As mentioned above, the plane with  $Z = H/2$  should satisfy the convection boundary condition expressed as Eq. (4). In this study,  $T_f = 573 \text{ K}$ . And the heat transfer coefficient is affected by the flow velocity, the viscosity and density of the coolant water. When the ‘lack of water’ accident happens, the heat transfer coefficient might degrade to a very low extent. So the effects of the variations of the heat transfer coefficients on the thermal performance of the fuel plate are investigated.

Fig. 2 depicts the finite element model of the fuel plate with particle volume fraction being 20%. The developed finite element models are different depending on different volume fractions, sizes and geometries of the particles.

The finite element model is discretized as 31 777 elements and 46 983 nodes, and the precision is satisfied. The mesh grid figure is shown as Fig. 2(c).

### 4. Results and discussions

In the finite element model of Fig. 2, the fuel particle is  $\text{UO}_2$  and the matrix is Zircaloy. In practice, other materials for the fuel particles and the matrix might be used. To adopt the above materials is partly for the reason that the needed material parameters might be obtained. The conductivity of  $\text{UO}_2$  is acquired according to Eq. (5), which is influenced by the burnup and the temperatures. The conductivity of Zircaloy acquired from Eq. (7) is also temperature-dependent. As a result, the non-linear computation should be performed to calculate the temperature field.

In this section, the non-linear calculation with Code ANSYS 10.0 for the finite element model is carried out. The effects of burnup,

surface heat transfer coefficients, heat generation rates of fuel particles and particle volume fractions on the temperature distribution are investigated; furthermore, the influences of the surface heat transfer coefficients, the particle volume fractions and the heat generation rates on the thermal flux of the plate surface are studied.

4.1. Effects of burnup on the temperature distribution

4.1.1. Effects of the degraded thermal conductivities of fuel particles due to burnup increase

In this case, the considered heat generation rate is  $3.204 \text{ W/mm}^3$ , the heat transfer coefficient between the fuel element and the coolant water is taken as  $h = 2 \times 10^4 \text{ W/m}^2 \text{ K}$  and the volume fraction of the fuel particles is 20%.

Due to the solid fission products and the gaseous fission products, the conductivities of the fuel particles degrade with increasing burnup [17]. The effects of the degraded conductivities of the fuel particles corresponding to burnup increase on the temperature variations are examined, shown as Fig. 3. Fig. 3 depicts the temperature variations along the export path (the line through the particle centers from the mid-plane to the outside surface) illustrated in Fig. 2. In Fig. 3, the results at line 6 correspond to an extreme case in which the relative conductivity is very low. It might be seen from Fig. 3 that with increasing burnup, (1) the internal temperatures of the fuel element rise; (2) the smooth extent reduces and the local heating phenomenon appears when the burnup arrives at a certain extent; (3) the temperature differences from the mid-plane to the outside surface gradually go up. As far as the actual values are concerned, the variations are not evident. In the range of the concerned parameters, the maximum increase of temperatures at the mid-plane is about 2 K.

The appearance of the above phenomena results from the fact that the thermal conductivities of the fuel particles decrease along with increasing burnup and the generated heat might not be taken out quickly. However, since the matrix material still occupies a larger part; the thermal conductivity of the dispersion element might remain higher, as a result, the temperature variation is slight.

4.1.2. Effects of the particle swelling together with degraded thermal conductivities and heat transfer coefficients

The heat generation rates, original volume fractions of the fuel particles and the surface temperature are the same to Section 4.1.1. Using the thermal conductivity model depicted in Section 2.2 and the particle swelling model shown as Section 2.4, the thermal–mechanical behaviors are firstly calculated, in which the used method is similar to the one in our previously published paper

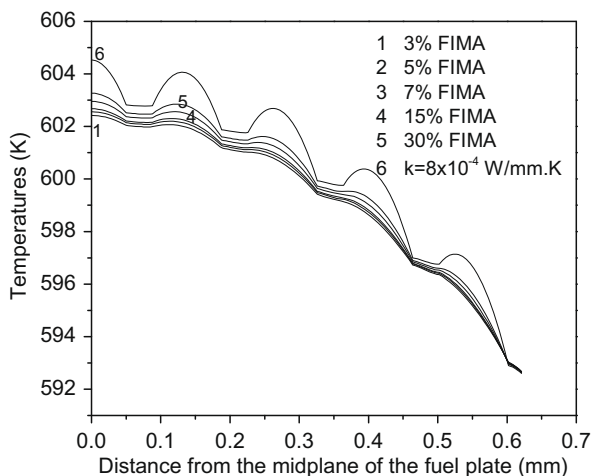


Fig. 3. The effects of the burnup on the temperature distribution.

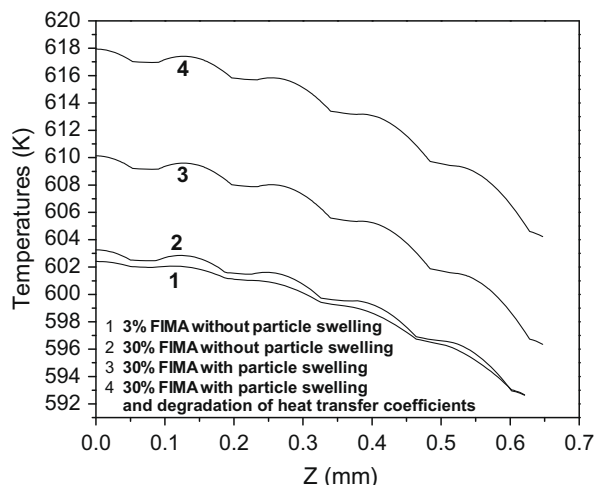


Fig. 4. The effects of particle swelling together with degraded thermal conductivity and heat transfer coefficients.

[22]. The deformation due to thermal expansion and particle swelling together with the mutual mechanical actions between the matrix and the fuel particle at 30% FIMA are obtained; also the actual volume variations, the deformed locations of the fuel particles and the thickness variation of the fuel plate are acquired. At 30% FIMA, the thickness of the fuel plate increases by  $52 \mu\text{m}$ ; compared to the original volume of the fuel particles, the particle volume increases by 19%; however, the new particle volume fraction is only 23% or so, so the metal matrix still occupies a large volume fraction.

Based on the deformed fuel plate, the new finite element model is developed, similar to Fig. 2(b), except that the sizes, locations of the fuel particles and the plate thickness are varied. The temperature field is investigated for two cases. For one case, the surface heat transfer coefficient is still  $2 \times 10^4 \text{ W/m}^2 \text{ K}$ ; for the other case, allowing for that the heat transfer coefficient might decrease due to the plate thickness increase, the used surface heat transfer coefficient is set as  $1.5 \times 10^4 \text{ W/m}^2 \text{ K}$ . The temperature distributions along the export path for the above two cases are denoted as lines 3 and 4 in Fig. 4. Compared with lines 1 and 2 without considering the particle swelling and plate deformations, it might be found that the internal temperatures of the fuel plate increase distinctly due to the volume expansion of the fuel particles; and the results with taking the degraded heat transfer coefficients into account are much larger. If the degraded thermal conductivities of the fuel particles are only considered, the internal temperature variations with increasing burnup are slight, as shown in line 1 and line 2 of Fig. 4. When the actual deformations are considered, the evident variations might be discovered, as shown in line 3; however, compared to the results at 3% FIMA, the temperature at the mid-plane of the fuel plate increases only 9 K or so, which is not too large. If the degraded heat transfer coefficient is also considered, the temperature at the mid-plane of the fuel plate increases about 16 K.

So, it might be obtained that the internal temperatures of the fuel plate increase more evidently at higher burnup with considering the particle swelling; but the variations of the concrete values are not too large for the metal matrix with higher thermal conductivities still occupying a main part; if the surface heat transfer coefficients are lowered largely, the internal temperatures might increase heavily.

4.2. Effects of surface heat transfer coefficients on the temperature distribution

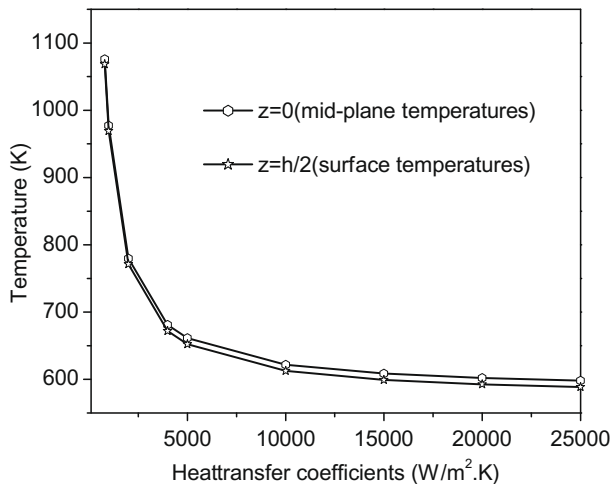
With increasing burnup, the volume swelling [2] of fuel particles might increase the thickness of the fuel plate. It might have



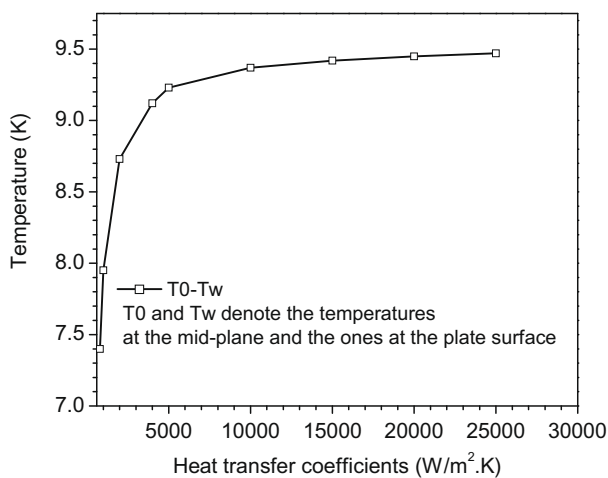
effects on the flow of the coolant and might result in degradation of the heat transfer coefficients at the convection boundary of the fuel plate. Other cases such as the 'Lack of Water' accident might also deduce this problem.

Under the conditions of unchanging the heat generation rate of the fuel particles and the temperature of the coolant water, the calculated temperatures at 1% FIMA for different heat transfer coefficients are revealed in Fig. 5.

It might be observed from Fig. 5 that the internal temperatures of the fuel plate might be sensitive to the decrease of the heat transfer coefficients when the values of the heat transfer coefficients arrive at about  $5 \times 10^3 \text{ W/m}^2 \text{ K}$ . When the heat transfer coefficients are lower than  $1 \times 10^3 \text{ W/m}^2 \text{ K}$ , the internal temperatures might ascend to the temperature higher than 1000 K. It might be also found that the internal temperatures of the fuel plate decrease with increasing heat transfer coefficients, nevertheless, when the heat transfer coefficients reach a certain extent, this effect is not distinct. Fig. 5(b) depicts the effects of the heat transfer coefficients on the temperature differences between the mid-plane and the outside surface. It might be discovered that the maximum temperature difference heightens with increasing the heat transfer



(a)



(b)

Fig. 5. The effects of the surface heat transfer coefficient on the temperature distribution. (a) The temperature distributions at the plate surface and the mid-plane and (b) the temperature differences between the mid-plane and the plate surface.

coefficients and this effect wears off when the heat transfer coefficients mount up to a certain extent.

Through the above quantitative research, it might be realized that low heat transfer coefficients are extremely bad to the security of the fuel plate.

#### 4.3. Effects of heat generation rates of the fuel particles on the temperature distribution

The temperatures at 1% FIMA along the export path with the heat generation rate being  $3.5 \text{ W/mm}^3$ ,  $4 \text{ W/mm}^3$ ,  $4.5 \text{ W/mm}^3$  and  $5 \text{ W/mm}^3$ , respectively, are shown in Fig. 6, and the other applied conditions are the same to the ones in Section 4.1.

It might be found from Fig. 6 that the internal temperatures of the fuel plate increase with increasing the heat generation rates and the temperature differences between the mid-plane and the outside surface turn larger gradually. When the heat generation rates increase from  $3.5 \text{ W/mm}^3$  to  $5 \text{ W/mm}^3$ , the mid-plane temperature of the fuel plate has a rise of 13.6 K, the temperature at the outside surface has a rise of 9.2 K and the temperature difference between the mid-plane and the outside surface has an increase of about 4 K. This demonstrates that the internal temperatures of the fuel plate might become higher if the heat energy cannot be taken outside by the coolant water in time in the case of high fission rates.

#### 4.4. Effects of particle volume fractions on the temperature distribution

The effects of the volume fractions of the fuel particles on the internal temperatures at 1% FIMA of the fuel plate are evaluated with other parameters and conditions identical with the ones in Section 4.1. The temperature results along the export path are illustrated in Fig. 7.

It is evident that the internal temperatures and the temperature differences between the mid-plane and the outside surface rise evidently with increasing particle volume fraction. For the fuel plate with the particle volume fraction being 30%, the mid-plane temperature and the surface temperature might increase 29.3 K and 19.2 K, respectively, compared with the fuel plate having a particle volume fraction of 10%, and the temperature difference between the mid-plane and the outside surface also increases more than 10 K. It is obvious that the particle volume fraction has a large effect on the internal temperatures of the fuel plate, which is primarily by the reason that the thermal conductivities of the fuel particles are lower compared to the Zircaloy matrix.

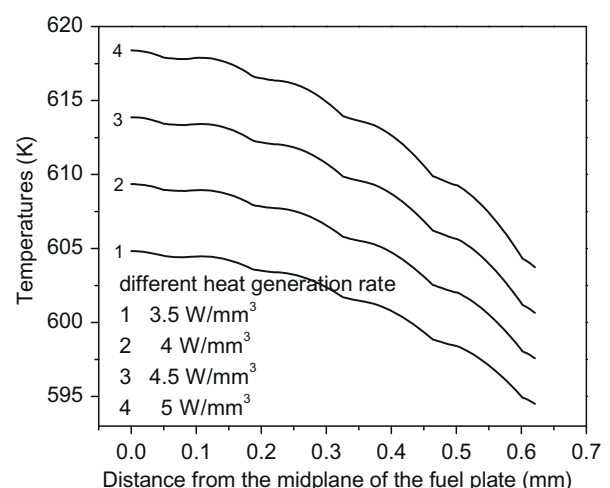


Fig. 6. The effects of heat generation rates on the temperature distribution at 1% FIMA.

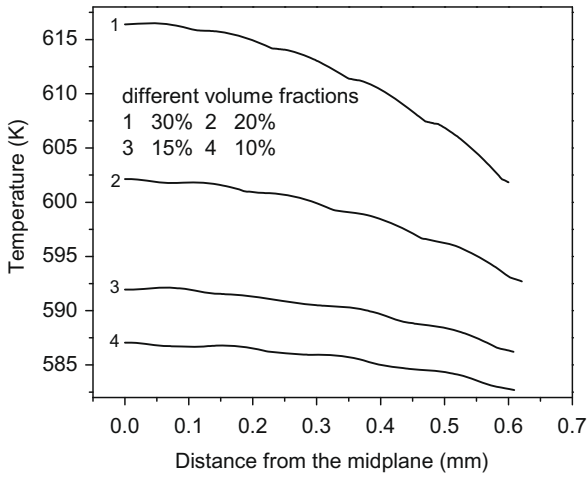


Fig. 7. The effects of particle volume fraction on the temperature distribution at 1% FIMA.

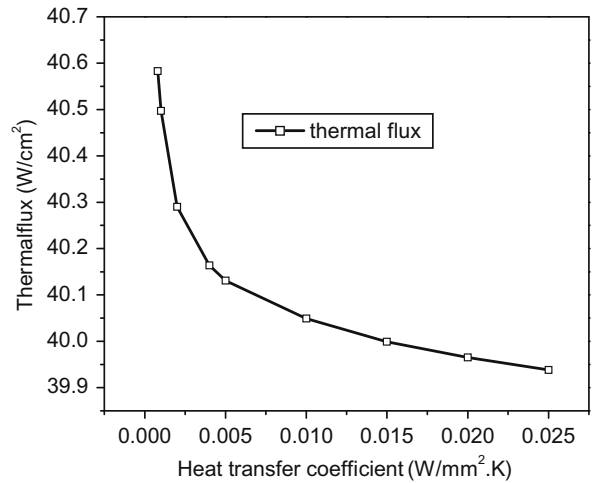
4.5. Effects of heat transfer coefficients, particle volume fractions and heat generation rates on the thermal flux of the outside surface

The thermal flux of the outside surface is mainly along the normal direction of the surface. It partly reflects the heat exchange effectiveness of the fuel element. Here the effects of different heat transfer coefficients, different particle volume fractions and different heat generation rates on the thermal flux are analyzed, as denoted in Fig. 8. It might be seen from Fig. 8(a) that the thermal fluxes decrease with increasing heat transfer coefficients, but the effect is slight in view of the actual values. It might be observed from Fig. 8(b) that the thermal flux of the outside surface distinctly rises up with increasing the volume fraction of the fuel particles. The thermal flux is three times larger with increasing the particle volume fraction from 10% to 30%. Furthermore, as might be seen from the slopes of the curves that the affecting extent intensifies with increasing particle volume fractions. As illustrated in Fig. 8(c), the effects of the heat generation rates are also very prominent and the relation between them take on an approximate linear relation. Increasing the heat generation rates from 3.5 W/mm<sup>3</sup> to 5 W/mm<sup>3</sup>, the thermal flux of the outside surface might increase 42.9%. As a whole, the increase of the heat transfer coefficients cannot lead to obvious variation of the thermal flux of the fuel element; on the contrary, increasing the particle volume fractions and heat generation rates might improve the thermal fluxes of the outside surface evidently.

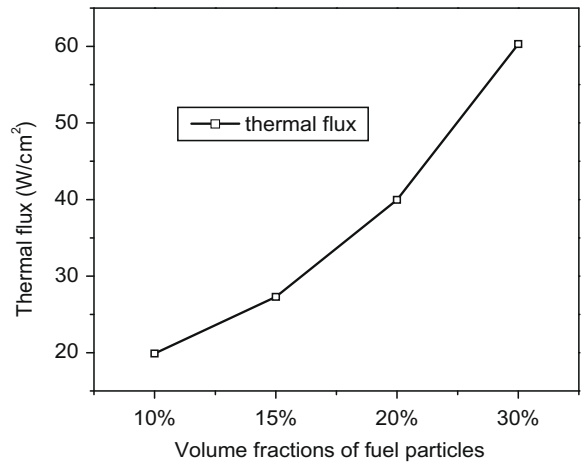
The above researches for the dispersion fuel plate not only give the effects of parametric variations on the internal temperatures and the thermal fluxes of the outside surface, but also lay a foundation for the further study of the thermal–mechanical behaviors.

5. Conclusions

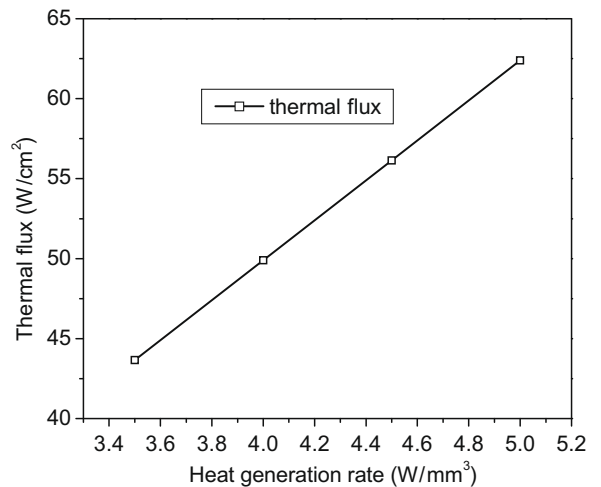
The metal-matrix dispersion fuel plate might be regarded as a kind of special particle composite, in which the particles are a fissile material that will generate heat energy and result in the internal heterogeneous temperature field. The boundary conditions of the upside and downside surfaces (the main boundaries of the fuel plate) might have important effects on the internal temperature field of the fuel plate. And the meso-structures of the dispersion fuels and the material parameters such as the degraded thermal conductivity might also influence the thermal performance of the fuel plate. Thus, it is necessary to model the thermal behaviors of



(a)



(b)



(c)

Fig. 8. The surface thermal flux at 1% FIMA affected by (a) different surface heat transfer coefficient (b) different particle volume fraction (c) different heat generation rate.

the dispersion fuel plate and carry out some parametric study to capture the affecting factors. And we hope that this study might be helpful to the fuel design and operation. The main conclusions are as follows:

- (1) A method of developing a special RVE for the dispersion fuel plate is developed. It might take account of the multi-particle circumstances of the dispersion fuels and reflect the mutual actions between the fuel particles and the matrix, besides, the main boundary conditions of the fuel plate are also considered.
- (2) The internal temperatures of the dispersion fuel plate rise up with increasing burnup and the local heating phenomenon appears when the thermal conductivities of the fuel particles degrade to an extreme case because of the increase of fission products with burnup. Although the thermal conductivities of the fuel particles decrease along with burnup, the internal temperatures of the fuel plate might not vary largely as long as the metal material of the matrix keep the original good value.
- (3) The internal temperatures of the fuel plate increase more evidently at higher burnup with considering the particle swelling; but the variations of the concrete values are not too large because the metal matrix with higher thermal conductivities still dominates the fuel element; if the surface heat transfer coefficients are lowered largely, the internal temperatures might increase heavily.
- (4) The internal temperatures and the maximum temperature differences go up with increasing the volume fractions and heat generation rates of the fuel particles. The heat transfer coefficients might have notable effects on the internal temperature; when their values are lower than a critical value the smaller decrease of the heat transfer coefficients might lead to very higher increase of the internal temperatures; increasing the heat transfer coefficients might decrease the internal temperatures, but this effect is not distinct when the heat transfer coefficients arrive at a certain extent. So the heat transfer coefficients seem to have an optimal value.
- (5) The thermal fluxes at the outside surface increase remarkably with increasing the volume fractions and heat generation rates of the fuel particles and decrease with increasing heat transfer coefficients. The effect of the heat transfer coefficient is slight.

### Acknowledgements

The authors are grateful for the supports of the Natural Science Foundation of China (Nos. 10772049 and 10672042), the Natural

Science Foundation of Shanghai (No. 06ZR14009), the Pujiang Scholar Program, the Natural Science Foundation of Shanghai post-doctor.

### References

- [1] P. Adelfang, I.N. Goldman, A.N. Soares, E. Bradley, in: Proceedings of the 28th International Meeting on Reduced Enrichment for Research and Test Reactors (RERTR), Cape Town, Republic of South Africa, October 29–November 2 2006.
- [2] Lee Van Duyn, Evaluation of the Mechanical Behavior of a Metal-matrix Dispersion Fuel for Plutonium Burning, Georgia Institute of Technology: A Thesis for the Degree Master of Science in Mechanical Engineering, 2003.
- [3] F. Huet, V. Marelle, J. Noirot, P. Sacristan, P. Lemoine, in: Proceedings of the 2003 International Meeting on Reduced Enrichment for Research and Test Reactors, Chicago, IL, 5–10 October 2003.
- [4] H.J. Ryu, Y.S. Han, J.M. Park, S.D. Park, C.K. Kim, J. Nucl. Mater. 321 (2003) 210.
- [5] A. Leenaers, S. Van den Berghe, E. Koonen, et al., J. Nucl. Mater. 335 (2004) 39.
- [6] F. Huet, J. Noirot, V. Marelle, S. Dubois, P. Boulcourt, P. Sacristan, S. Naury, P. Lemoine, in: Proceedings of the Ninth International Topical Meeting on Research Reactor Fuel Management, Budapest, Hungary, 10–13 April 2005.
- [7] J. Rest, G. Hofman, Nucl. Technol. 126 (1999) 88.
- [8] H. Taboada, J. Rest, M.V. Moscarda, M. Markiewicz, E. Estevez, in: Proceedings of the 24th International Management on Reduced Enrichment for Research and Test Reactors, San Carlos de Bariloche, Argentina, 3–8 November 2002.
- [9] J. Rest, The DART Dispersion Analysis Research Tool: A Mechanistic Model for Predicting Fission-Product-Induced Swelling of Aluminum Dispersion Fuels, ANL-95/36, 1995.
- [10] S.L. Hayes, M.K. Meyer, G.L. Hofman, J.L. Snelgrove, R.A. Brazener, in: Proceedings of the 2003 International Meeting on Reduced Enrichment for Research and Test Reactors, Chicago, IL, 5–10 October 2003.
- [11] S.L. Hayes, G.L. Hofman, M.K. Meyer, J. Rest, J.L. Snelgrove, in: 2002 International Meeting on Reduced Enrichment for Research and Test Reactors, Bariloche, Argentina, 3–8 November 2002.
- [12] V. Marelle, S. Dubois, M. Ripert, J. Noirot, P. Lemoine, in: The RERTR-2007 International Meeting on Reduced Enrichment for Research and Test Reactors, 23–27 September, Diplomat Hotel – Prague, Prague, Czech Republic, 2007.
- [13] V. Marelle, F. Huet, P. Lemoine, in: Proceedings of the Eighth International Topical Meeting on Research Reactor Fuel Management, München, Germany, 21–24 March 2004.
- [14] Roberto Saliba, Horacio Taboada, Ma. Virginia Moscarda, in: 2003 International Meeting on Reduced Enrichment for Research and Test Reactors, Chicago, IL, 5–10 October 2003.
- [15] P.G. Lucuta, H.S. Matzke, I.J. Hastings, J. Nucl. Mater. 232 (1996) 166.
- [16] MATPRO-09, A Handbook of Materials Properties for Use in the Analysis of Light Water Reactor Fuel Rod Behavior, USNRC TREE NUREG-1005, 1976.
- [17] W. Chubb, V.W. Storhok, D.L. Keller, Nucl. Technol. 18 (1973) 231.
- [18] T. Nakajima, M. Ichikawa, et al., FEMAXI-III: A Computer Code for the Analysis of Thermal and Mechanical Behavior of Fuel Rods, AERI-1298, 1985.
- [19] W. Wiesenack, M. Vankeerberghen, R. Thankappan, Assessment of UO<sub>2</sub> Conductivity Degradation Based on In-pile Temperature Data, HWR-469, 1996.
- [20] Harald Berger, Sreedhar Kari, Ulrich Gabbert, et al., Mater. Sci. Eng. A 412 (2005) 53.
- [21] Sreedhar Kari, Harald Berger, Reinaldo Rodriguez-Ramos, Ulrich Gabbert, Compos. Struct. 77 (2007) 223.
- [22] S.R. Ding, X. Jiang, Y.Z. Huo, L.A. Li, J. Nucl. Mater. 374 (3) (2008) 453.